

Many-body echo

Yang-Yang Chen,^{1,2} Pengfei Zhang,³ Wei Zheng^④,⁴ Zhigang Wu^④,^{1,*} and Hui Zhai^④,^{3,5,†}¹*Shenzhen Institute for Quantum Science and Engineering, and Department of Physics, Southern University of Science and Technology, Shenzhen 518055, China*²*CAS Key Laboratory of Quantum Information, University of Science and Technology of China, Hefei 230026, China*³*Institute for Advanced Study, Tsinghua University, Beijing, 100084, China*⁴*Hefei National Laboratory for Physical Sciences at Microscale and Department of Modern Physics, University of Science and Technology of China, Hefei 230026, China*⁵*Center for Quantum Computing, Peng Cheng Laboratory, Shenzhen 518055, China*

(Received 9 October 2019; accepted 16 June 2020; published 8 July 2020)

In this Rapid Communication, we propose a protocol to reverse a quantum many-body dynamic process. We name it “many-body echo” because the underlying physics is closely related to the spin echo effect in nuclear magnetic resonance systems. We consider a periodical modulation of the interaction strength in a weakly interacting Bose condensate, which resonantly excites quasiparticles from the condensate. A dramatic phenomenon is that, after pausing the interaction modulation for half a period and then continuing on with the same modulation, nearly all the excited quasiparticles in the resonance modes will be absorbed back into the condensate. During the intermediate half-period, the free evolution introduces a π phase, which plays a role reminiscent of that played by the π pulse in the spin echo. Comparing our protocol with another one implemented by the Chicago group in a recent experiment, we find that ours is more effective at reversing the many-body process. The difference between these two schemes manifests the physical effect of the micromotion in the Floquet theory.

DOI: [10.1103/PhysRevA.102.011301](https://doi.org/10.1103/PhysRevA.102.011301)

How to reverse a quantum many-body dynamic process is a question of great interest, especially in recent discussions of quantum many-body chaos and quantum information scrambling [1–3]. Ultracold atomic gases provide a unique platform to address these kinds of questions because of the following two reasons. First, unlike other artificial quantum systems such as nuclear magnetic resonance (NMR) and trapped ions, where the number of qubits is currently limited to below a few hundreds, ultracold atomic gases are many-body systems containing a macroscopically large number of quantum particles. Second, in contrast to electronic systems in condensed matter materials where phonons are inevitably present and will cause decoherence and dissipation, ultracold atomic gases are isolated systems whose coherence times can be much longer than typical timescales of condensed matter systems.

One type of dynamics that has been widely explored in ultracold atoms is that under periodical driving [4]. For instance, the periodical modulation of optical lattices has been employed to create artificial magnetic fields [5–13] and topological bands [14–23] and to realize gauge field with dynamics [24–26]. Recently, the Chicago group has explored the periodical modulation of the interacting strength between atoms in a weakly interacting Bose-Einstein condensate confined in a cylindrical box potential [27,28]. Such a modulation induces a parametric resonance and leads to an

exponential growth of quasiparticles with energy close to half the modulation frequency [29]. To show that this many-body dynamics is indeed coherent, in a recent experiment they also attempted to reverse it by inverting the time dependence of the interaction modulation [30]. To be more precise, the following time-dependent interaction strength $g(t)$ was considered:

$$g(t) = \begin{cases} g_0 \sin(\omega t) & 0 \leq t \leq nT \\ g_0 \sin(\omega t - \pi) & nT \leq t \leq 2nT, \end{cases} \quad (1)$$

where g_0 is the oscillation amplitude, ω is the oscillation frequency, $T = 2\pi/\omega$ is the period, and n is an integer. This oscillation scheme is denoted by protocol (a) and shown in Fig. 1(a). During the first n periods of oscillations $0 \leq t \leq nT$, atoms are resonantly excited to states whose energy are in the vicinity of $\hbar\omega/2$. In the second n periods of oscillations $nT \leq t \leq 2nT$, however, a significant portion of those excitations are found to return to the condensate mode. This is a strong evidence that a coherent many-body dynamic process can indeed be reversed.

In this Rapid Communication, we present a different oscillation scheme, denoted as the protocol (b) and shown in Fig. 1(b), which we show can reverse the many-body dynamics to a greater degree than the protocol (a). This scheme is mathematically described by

$$g(t) = \begin{cases} g_0 \sin(\omega t) & 0 \leq t \leq nT \\ 0 & nT \leq t \leq (n + \frac{1}{2})T \\ g_0 \sin(\omega t - \pi) & (n + \frac{1}{2})T \leq t \leq (2n + \frac{1}{2})T. \end{cases} \quad (2)$$

*wuzg@sustech.edu.cn

†hzhai@tsinghua.edu.cn

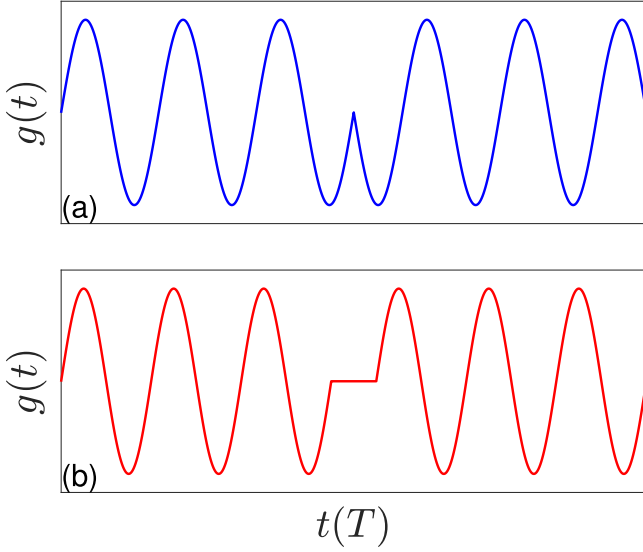


FIG. 1. The time dependence of the interaction strength. (a) Protocol used in the Chicago experiment and (b) protocol proposed in this Rapid Communication.

In this scheme, the driving takes a half-period break after the first n periods of oscillation, whereby the system undergoes free evolution governed by the noninteracting Hamiltonian. The second n period of oscillation is a repetition of the first, which can be seen by letting $t' = t - T/2$ and writing $g(t') = g_0 \sin(\omega t')$ for $nT \leq t' \leq 2nT$. Without the half period pause inserted in between, we would simply have a single oscillation throughout the entire process and the quasiparticles will be continuously excited. Thus, the fact that our scheme can reverse the quasiparticle excitation process is quite counter-intuitive at first glance.

As we will explain in detail later, the underlying principle by which the protocol (b) reverses the dynamics is reminiscent of the spin echo [31,32]. Spin echo in a NMR system is a scheme to refocus the magnetization against the dephasing due to the inhomogeneous magnetic field. There, the magnetic field under which the spins precess does not change, similar to the fact that our protocol (b) involves exactly the same modulation $g(t)$ in the first and second n periods of driving. The key of the spin echo effect is a π pulse during the spin precession that inverts the spin orientation. In our protocol (b), the analogy of the π pulse is the free evolution that introduces a phase to the wave function. Because of this close analogy with the spin echo and the many-body nature of our problem, we refer to the dynamics under our protocol as the “many-body echo.”

Bogoliubov theory. We consider a Bose gas with a periodically modulated interaction, described by the Hamiltonian

$$\hat{H} = \int d\mathbf{r} \hat{\psi}^\dagger(\mathbf{r}) \left[-\frac{\hbar^2 \nabla^2}{2m} + V_{\text{tr}}(\mathbf{r}) \right] \hat{\psi}(\mathbf{r}) + \frac{g(t)}{2} \int d\mathbf{r} \hat{\psi}^\dagger(\mathbf{r}) \hat{\psi}^\dagger(\mathbf{r}) \hat{\psi}(\mathbf{r}) \hat{\psi}(\mathbf{r}), \quad (3)$$

where $\hat{\psi}(\mathbf{r})$ is the bosonic field, $V_{\text{tr}}(\mathbf{r})$ is the trapping potential, m is the atom mass, and $g(t)$ is the interaction strength. At $t = 0$, the system is noninteracting and all the particles are

condensed in the ground state $\varphi_0(\mathbf{r})$ of the single-particle Hamiltonian $\hat{h}(\mathbf{r}) = -\hbar^2 \nabla^2 / (2m) + V_{\text{tr}}(\mathbf{r})$. After the interaction modulation is turned on, we monitor the dynamics by calculating the population on the single particle excited state $\varphi_j(\mathbf{r})$, where $\hat{h}(\mathbf{r})\varphi_j(\mathbf{r}) = \epsilon_j \varphi_j(\mathbf{r})$. We focus on a regime where the dynamics can be well captured by the following time-dependent Bogoliubov–de Gennes (BdG) equations [33]:

$$i\hbar \partial_t u_j(\mathbf{r}, t) = \mathcal{L}(\mathbf{r}, t) u_j(\mathbf{r}, t) - g(t) \Phi_0^{*2} v_j(\mathbf{r}, t), \quad (4)$$

$$i\hbar \partial_t v_j(\mathbf{r}, t) = -\mathcal{L}(\mathbf{r}, t) v_j(\mathbf{r}, t) + g(t) \Phi_0^{*2} u_j(\mathbf{r}, t), \quad (5)$$

where the Bogoliubov amplitudes satisfy the orthonormality relations $\int d\mathbf{r} [u_i(\mathbf{r}, t) u_j^*(\mathbf{r}, t) - v_i(\mathbf{r}, t) v_j^*(\mathbf{r}, t)] = \delta_{ij}$ with the initial conditions $u_i(\mathbf{r}, 0) = \varphi_i(\mathbf{r})$ and $v_i(\mathbf{r}, 0) = 0$. Here $\mathcal{L}(\mathbf{r}, t) \equiv \hat{h}(\mathbf{r}) + 2g(t)|\Phi_0(\mathbf{r}, t)|^2 - \mu$, where μ is the initial chemical potential and $\Phi_0(\mathbf{r}, t) = \sqrt{N_0(t)}\varphi_0(\mathbf{r})$ is the time-dependent condensate wave function. The number of particles excited to the state $\varphi_j(\mathbf{r})$ is given by $N_j(t) = \int d\mathbf{r} |v_j(\mathbf{r}, t)|^2$. Equations (4) and (5) are solved together with number conservation condition $N = N_0(t) + \sum_j N_j(t)$. The validity of the BdG theory requires that the number of excitations should be relatively small, which is satisfied by all the calculations in our study.

To illustrate the essential physics involved, we first consider a uniform condensate and, for simplicity, take the condensate density $|\Phi_0(\mathbf{r}, t)|^2$ to be a constant n_0 independent of time. This approximation is not necessary for the numerical calculation but will simplify our later analysis without compromising the main results. As mentioned earlier, a periodical modulation of the interaction with frequency ω mostly excites the atoms to states with energy $\epsilon_{\mathbf{k}} \equiv \hbar^2 \mathbf{k}^2 / (2m) \sim \hbar\omega/2$, because two atoms with opposite momentum collide and absorb one quanta of energy $\hbar\omega$. Shown in Fig. 2 are the population of atoms excited to the resonant energy $\epsilon_{\mathbf{k}} = \hbar\omega/2$ and to a slightly modified resonant energy $\epsilon_{\mathbf{k}} = (1/2 + 3\gamma^2/8)\hbar\omega$ (the significance of this modification will be explained later), calculated for the interaction modulations depicted in both protocols (a) and (b). Here $\gamma = g_0 n_0 / (\hbar\omega)$ is a relatively small, dimensionless parameter that characterizes the strength of the modulation. As we can see, for both schemes, the atoms are excited during the first stage of interaction modulation, but most of them are absorbed back to condensate after the second stage. It is also clear that the protocol (b) reverses the many-body process much better than the protocol (a), particularly for larger modulation strengths.

Floquet Hamiltonian. We first present our understanding of the above phenomenon in terms of the Floquet Hamiltonian, which governs the stroboscopic evolution of the system. We begin with the Bogoliubov Hamiltonian for the uniform condensate $\hat{H}_{\text{Bg}}(t) = g(t)N^2/(2V) + \sum_{\mathbf{k}} \hat{H}_{\text{Bg}}^{\mathbf{k}}(t)$, where V is the volume and

$$\hat{H}_{\text{Bg}}^{\mathbf{k}}(t) = [\epsilon_{\mathbf{k}} + g(t)n_0] \hat{a}_{\mathbf{k}}^\dagger \hat{a}_{\mathbf{k}} + \frac{n_0 g(t)}{2} (\hat{a}_{\mathbf{k}}^\dagger \hat{a}_{-\mathbf{k}}^\dagger + \text{H.c.}). \quad (6)$$

To derive the Floquet Hamiltonian using the high-frequency expansion, it is necessary to first apply the rotating frame transformation

$$\hat{R}(t) = \exp \left(\frac{i\omega t}{2} \sum_{\mathbf{k} \neq 0} \hat{a}_{\mathbf{k}}^\dagger \hat{a}_{\mathbf{k}} \right) \quad (7)$$

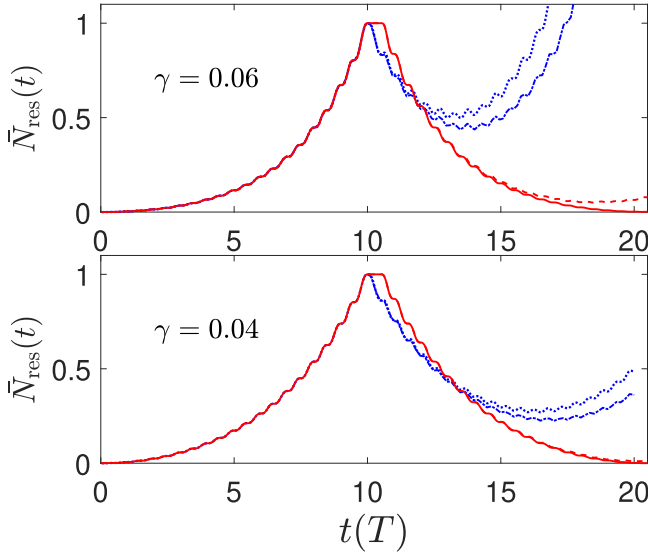


FIG. 2. Normalized population of resonant excitations as a function of time from both protocol (a) (red, solid, and dashed) and protocol (b) (blue, dash-dotted and dotted) depicted in Fig. 1. The dashed and dotted lines are the populations at $\epsilon_{\mathbf{k}} = \hbar\omega/2$ and the solid and dash-dotted lines are those at $\epsilon_{\mathbf{k}} = (1/2 + 3\gamma^2/8)\hbar\omega$. Calculations are done for two values of modulation strength, i.e., $\gamma = 0.06$ in the upper panel and $\gamma = 0.04$ in the lower panel.

to eliminate the resonance energy term. In doing so, the Hamiltonian in the rotating frame is given by $\hat{H}_R(t) = \hat{R}(t)[\hat{H}_{Bg}(t) - i\hbar\partial_t]\hat{R}^\dagger(t)$, which yields $\hat{H}_R(t) = g(t)N^2/(2V) + \sum_{\mathbf{k}} \hat{H}_R^{\mathbf{k}}(t)$ with

$$\hat{H}_R^{\mathbf{k}}(t) = \left[\epsilon_{\mathbf{k}} - \frac{\hbar\omega}{2} + g(t)n_0 \right] \hat{a}_{\mathbf{k}}^\dagger \hat{a}_{\mathbf{k}} + \frac{g(t)n_0}{2} (e^{i\omega t} \hat{a}_{\mathbf{k}}^\dagger \hat{a}_{-\mathbf{k}}^\dagger + e^{-i\omega t} \hat{a}_{\mathbf{k}} \hat{a}_{-\mathbf{k}}). \quad (8)$$

For an interaction strength $g(t)$ periodical in T , an effective Floquet Hamiltonian \hat{H}_{eff} capturing the evolution at integer periods of oscillation can be introduced by

$$\mathcal{T} \exp\left(-\frac{i}{\hbar} \int_{\alpha T}^{\alpha T+T} \hat{H}_R(t) dt\right) = \exp\left(-\frac{i}{\hbar} \hat{H}_{\text{eff}} T\right), \quad (9)$$

where \mathcal{T} is the time-ordering operator and α specifies the initial reference time. By Fourier transforming $\hat{H}_R(t) = \sum_p \hat{H}_p e^{ip\omega t}$ and using the $1/\omega$ expansion, we obtain [34]

$$\hat{H}_{\text{eff}} \approx \hat{H}_0 + \sum_{p>0} \left(\frac{[\hat{H}_p, \hat{H}_{-p}]}{p\hbar\omega} - \frac{[\hat{H}_p, \hat{H}_0]}{p\hbar\omega e^{-i2p\alpha\pi}} + \frac{[\hat{H}_{-p}, \hat{H}_0]}{p\hbar\omega e^{i2p\alpha\pi}} \right). \quad (10)$$

The effective Floquet Hamiltonian we define here is different from the conventional one [35,36], in which the information of the initial state is absorbed in the kick operator.

For $0 \leq t \leq nT$, the time dependence of $g(t)$ is the same for protocols (a) and (b). Writing $\hat{H}_{\text{eff}} = \sum_{\mathbf{k}} \hat{H}_{\text{eff}}^{\mathbf{k}}$ and following Eq. (10), we obtain for this duration

$$\frac{\hat{H}_{\text{eff}}^{\mathbf{k}}}{\hbar\omega} = -\frac{1}{2} \gamma \hat{A}_y^{\mathbf{k}} - \gamma^2 \hat{A}_x^{\mathbf{k}} + \Delta_{\mathbf{k}} (\hat{A}_z^{\mathbf{k}} - 1/2), \quad (11)$$

where $\Delta_{\mathbf{k}} \equiv \epsilon_{\mathbf{k}}/\hbar\omega - 1/2 - 3\gamma^2/8$ and

$$\begin{aligned} \hat{A}_x^{\mathbf{k}} &\equiv \frac{1}{2} (\hat{a}_{\mathbf{k}}^\dagger \hat{a}_{-\mathbf{k}}^\dagger + \hat{a}_{\mathbf{k}} \hat{a}_{-\mathbf{k}}), \\ \hat{A}_y^{\mathbf{k}} &\equiv \frac{1}{2i} (\hat{a}_{\mathbf{k}}^\dagger \hat{a}_{-\mathbf{k}}^\dagger - \hat{a}_{\mathbf{k}} \hat{a}_{-\mathbf{k}}), \\ \hat{A}_z^{\mathbf{k}} &\equiv \frac{1}{2} (\hat{a}_{\mathbf{k}}^\dagger \hat{a}_{\mathbf{k}} + \hat{a}_{-\mathbf{k}} \hat{a}_{-\mathbf{k}}^\dagger). \end{aligned}$$

These three operators form the group of pseudorotations, $SU(1,1)$, obeying the commutation relations $[\hat{A}_x^{\mathbf{k}}, \hat{A}_y^{\mathbf{k}}] = -i\hat{A}_z^{\mathbf{k}}$, $[\hat{A}_y^{\mathbf{k}}, \hat{A}_z^{\mathbf{k}}] = i\hat{A}_x^{\mathbf{k}}$, and $[\hat{A}_z^{\mathbf{k}}, \hat{A}_x^{\mathbf{k}}] = i\hat{A}_y^{\mathbf{k}}$.

The second n periods of oscillation in the protocols (a) and (b) are governed by different Floquet Hamiltonians. For protocol (a), we find the following effective Hamiltonian,

$$\frac{\hat{H}_{\text{eff},a}^{\mathbf{k}}}{\hbar\omega} = \frac{1}{2} \gamma \hat{A}_y^{\mathbf{k}} - \gamma^2 \hat{A}_x^{\mathbf{k}} + \Delta_{\mathbf{k}} (\hat{A}_z^{\mathbf{k}} - 1/2), \quad (12)$$

for $nT \leq t \leq 2nT$. If we consider the resonant modes $\epsilon_{\mathbf{k}} \sim \hbar\omega/2$ such that $\Delta_{\mathbf{k}} \sim 3\gamma^2/8$, it is clear that $\hat{H}_{\text{eff},a}^{\mathbf{k}}$ inverts $\hat{H}_{\text{eff}}^{\mathbf{k}}$ up to the leading order of γ , but not to the second order of γ^2 .

Now consider the protocol (b). During the half period of free evolution $nT \leq t \leq (n+1/2)T$, the Hamiltonian in the rotating frame vanishes for the resonant modes with $\epsilon_{\mathbf{k}} \sim \hbar\omega/2$. For $nT + T/2 \leq t \leq 2nT + T/2$, even though the functional form of $g(t)$ is the same as that in the second stage of protocol (a), the initial reference time characterized by parameter α in Eq. (9) is different. More specifically, we have $\alpha = 0$ for the protocol (a) and $\alpha = 1/2$ for the protocol (b). In the Floquet theory, this results in a difference in the so-called micromotion term in the effective Hamiltonian [35]. Thus, we find the effective Hamiltonian of the protocol (b) as

$$\frac{\hat{H}_{\text{eff},b}^{\mathbf{k}}}{\hbar\omega} = \frac{1}{2} \gamma \hat{A}_y^{\mathbf{k}} + \gamma^2 \hat{A}_x^{\mathbf{k}} + \Delta_{\mathbf{k}} (\hat{A}_z^{\mathbf{k}} - 1/2) \quad (13)$$

for $nT + T/2 \leq t \leq 2nT + T/2$. Now we can see that both the first and second terms in $\hat{H}_{\text{eff},b}^{\mathbf{k}}$ are opposite to those in $\hat{H}_{\text{eff}}^{\mathbf{k}}$. If we further consider the resonance modes specified by $\Delta_{\mathbf{k}} = 0$, i.e., $\epsilon_{\mathbf{k}} = (1/2 + 3\gamma^2/8)\hbar\omega$, $\hat{H}_{\text{eff},b}^{\mathbf{k}}$ completely inverts $\hat{H}_{\text{eff}}^{\mathbf{k}}$ for all contributions up to the order of γ^2 . This explains why the protocol (b) reverses the many-body dynamic process better than the protocol (a). Since the difference between the two protocols lies in the second-order terms of γ in the effective Hamiltonian, it also explains why the difference is more significant for larger γ , as shown in Fig. 2. Finally, it can be shown that all the excitations with $\Delta_{\mathbf{k}} \ll \gamma$ will be well reversed by our protocol.

Many-body echo. Now we discuss the connection between the underlying physics of the protocol (b) and the spin echo. For this purpose, we introduce an alternative approach to understand the reversal of dynamics. As mentioned earlier, the first and second n periods of oscillation in the protocol (b) are identical, which can be seen by writing $t' = t - T/2$, such that $g(t') = g_0 \sin(\omega t')$ for $nT \leq t' \leq 2nT$. However, they become inequivalent when viewed from the single rotating frame of reference introduced, leading to different Floquet Hamiltonians obtained earlier. Such an equivalence can be restored if we apply the unitary rotation $\hat{R}(t)$ for $0 \leq t \leq nT$ and another $\hat{R}(t')$ for $nT \leq t' \leq 2nT$ (i.e. $nT + T/2 \leq t \leq 2nT + T/2$). In this approach, the free evolution for the

intermediate half period $nT \leq t \leq nT + T/2$ is according to the original Bogoliubov Hamiltonian in Eq. (6), but the system will be governed by the same effective Hamiltonian \hat{H}_{eff} in Eq. (11) during both sections of the driving. Hence, the total evolution operator from $t = 0$ to $t = 2nT + T/2$ is given by

$$\hat{U} = \hat{R}^\dagger(2nT)e^{-\frac{i}{\hbar}\hat{H}_{\text{eff}}nT}\hat{R}(nT) \times e^{-i\frac{T}{2\hbar}\sum_{\mathbf{k}}\epsilon_{\mathbf{k}}\hat{a}_{\mathbf{k}}^\dagger\hat{a}_{\mathbf{k}}}\hat{R}^\dagger(nT)e^{-\frac{i}{\hbar}\hat{H}_{\text{eff}}nT}\hat{R}(0). \quad (14)$$

Restricting ourselves to resonance modes with $\epsilon_{\mathbf{k}} \sim \hbar\omega/2$ and using $\hat{R}(nT) = (-1)^n$, we obtain $\hat{U} = \prod_{\mathbf{k}}' \hat{U}_{\mathbf{k}}$, where

$$\hat{U}_{\mathbf{k}} = e^{-\frac{2i}{\hbar}\hat{H}_{\text{eff}}nT} e^{-i\pi\hat{A}_{\mathbf{k}}^z} e^{-\frac{2i}{\hbar}\hat{H}_{\text{eff}}nT}. \quad (15)$$

Here $\prod_{\mathbf{k}}'$ restricts the product over \mathbf{k} to half momentum space. The operator $e^{-i\pi\hat{A}_{\mathbf{k}}^z}$ is reminiscent of the π pulse inserted in the spin echo experiment. More precisely, this operator acts on the Bogoliubov-type many-body state as

$$e^{-i\pi\hat{A}_{\mathbf{k}}^z} e^{(\chi_{\mathbf{k}}\hat{a}_{\mathbf{k}}^\dagger\hat{a}_{-\mathbf{k}}^\dagger - \chi_{\mathbf{k}}^*\hat{a}_{\mathbf{k}}\hat{a}_{-\mathbf{k}})}|0\rangle = e^{-(\chi_{\mathbf{k}}\hat{a}_{\mathbf{k}}^\dagger\hat{a}_{-\mathbf{k}}^\dagger - \chi_{\mathbf{k}}^*\hat{a}_{\mathbf{k}}\hat{a}_{-\mathbf{k}})}|0\rangle.$$

We note that this operator adds a π phase shift to the wave function of excitations, which plays a key role in reversing the many-body dynamics.

Harmonically trapped case. For the uniform system, the resonance of excitations due to the interaction modulation has a typical width of the order of $\gamma\hbar\omega$, while our protocol only reverses those satisfying $|\epsilon_{\mathbf{k}} - \hbar\omega/2| \ll \gamma\hbar\omega$. In order to achieve a complete reversal of all excitations, we turn to a Bose condensate confined in a harmonic trap. The advantage of this setup is that the mode energy of the harmonic trap is discrete; thus only pairs of particles whose total energy is resonant with $\hbar\omega$ can be excited, provided that the mode level separation is large than the amplitude of interaction modulation. In such scenarios, almost all the excitations can be reversed by our protocol.

Without loss of generality, we consider an elongated condensate with transverse and axial trapping frequencies as $\omega_{\perp} = 2\pi \times 430$ Hz and $\omega_z = 2\pi \times 200$ Hz respectively. Here we specifically choose two incommensurate values for ω_{\perp} and ω_z . In this way, when the interaction modulation frequency is chosen to be commensurate with ω_z , only the axial modes $\epsilon_j = (j + 1/2)\hbar\omega_z$ meeting the resonance condition $(i + j)\omega_z = \omega$ will be excited. Thus, as far as the dynamics is concerned, the Hamiltonian of the system can be reduced to a one-dimensional one with an effective interaction modulation amplitude $\tilde{g}_0 = g_0/(2\pi l_{\perp}^2)$, where $l_{\perp} = \sqrt{\hbar/m\omega_{\perp}}$ [37]. We numerically solve the number-conserving BdG equations described earlier for this system with a total atom number $N = 1800$ and a modulation frequency $\omega = 20\omega_z$. For these parameters, the modulation strength is $\tilde{\gamma} = \frac{g_0\tilde{n}_0}{\hbar\omega} = 0.12$, where $\tilde{n}_0 = N/l_z$ with $l_z = \sqrt{\hbar/m\omega_z}$. Shown in Fig. 3 are the total number of excitations $N_{\text{tot}}(t) = \sum_j N_j(t)$. We see that our protocol, again much more effective than the protocol (a), achieves an almost perfect reversal of all the excitations. Lastly, we have verified that the many-body echo phenomenon is rather robust against variations of system parameters as long as the resonance condition is satisfied [37].

Outlook. In summary, we have developed an analogy of the spin echo in a Floquet quantum many-body system, which we refer to as the many-body echo. Although here

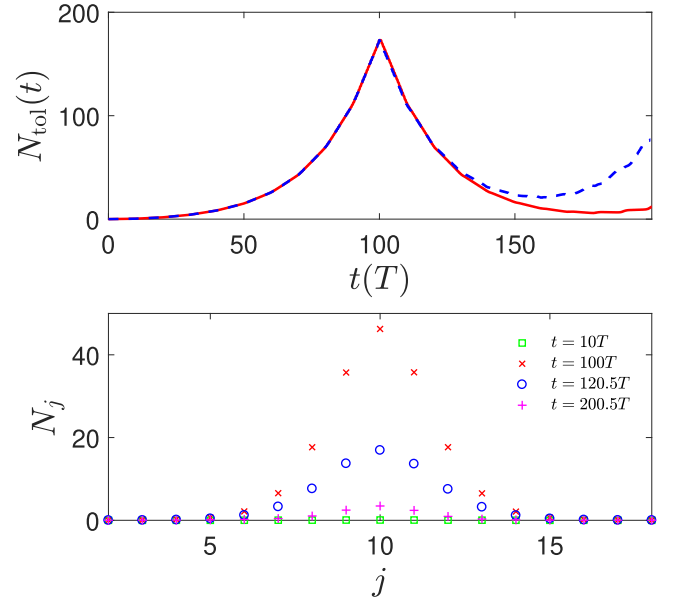


FIG. 3. Upper panel: the total number of excitations as a function of time in a trapped condensate with total number of atoms $N = 1800$. The dashed (blue) line and the solid (red) line correspond to the protocol (a) and protocol (b) respectively. Lower panel: the occupation of different single-particle modes at different times for protocol (b).

we demonstrate many-body echo using a weakly interacting Bose condensate as an example, the idea can be applied universally to scenarios of resonant excitation in Floquet systems. Consider a driving with frequency ω that resonantly excites the system to many-body states with energy $\Delta E = \omega$. By pausing the driving for half a period, a phase difference $e^{i\Delta E \times T/2} = e^{i\omega \times T/2} = e^{i\pi}$ accumulates between these states and the ground state. Such a phase is reminiscent of the π rotation in spin echo and is ultimately responsible for the reversal of dynamics. Thus, we believe that this physical picture can find broad applications in future research of Floquet quantum matter. One application, for instance, could be facilitating the experimental measurement of the out-of-time-ordered correlation function by reversing the many-body dynamics [38–40]. Another application draws inspiration from the spin-echo effect, where the imperfect refocusing can be used to detect decoherence time due to spin-spin interactions. Similarly, in a many-body system with significant quasiparticle interactions, the degree to which our protocol does not reverse the dynamics can then be attributed to the quasiparticle interactions, the treatment of which requires more sophisticated theoretical methods [41–43].

Acknowledgments. Y.-Y.C. is supported by the China Postdoctoral Science Foundation (Grant No. 2019M650145) and Sustech Presidential Postdoctoral Fellowship. Z.W. acknowledge support by NSFC (Grant No. 11974161) and Key-Area Research and Development Program of Guangdong Province (Grant No. 2019B030330001). H.Z. acknowledges support from the Beijing Outstanding Young Scientist Program, MOST (Grant No. 2016YFA0301600) and NSFC (Grant No. 11734010).

- [1] E. Altman, *Nat. Phys.* **14**, 979 (2018).
- [2] X.-L. Qi, *Nat. Phys.* **14**, 984 (2018).
- [3] B. Swingle, *Nat. Phys.* **14**, 988 (2018).
- [4] A. Eckardt, *Rev. Mod. Phys.* **89**, 011004 (2017).
- [5] J. Struck, C. Ölschläger, R. Le Targat, P. Soltan-Panahi, A. Eckardt, M. Lewenstein, P. Windpassinger, and K. Sengstock, *Science* **333**, 996 (2011).
- [6] M. Aidelsburger, M. Atala, S. Nascimbene, S. Trotzky, Y.-A. Chen, and I. Bloch, *Phys. Rev. Lett.* **107**, 255301 (2011).
- [7] J. Struck, C. Ölschläger, M. Weinberg, P. Hauke, J. Simonet, A. Eckardt, M. Lewenstein, K. Sengstock, and P. Windpassinger, *Phys. Rev. Lett.* **108**, 225304 (2012).
- [8] J. Struck, M. Weinberg, C. Ölschläger, P. Windpassinger, J. Simonet, K. Sengstock, R. Höppner, P. Hauke, A. Eckardt, M. Lewenstein, and L. Mathey, *Nat. Phys.* **9**, 738 (2013).
- [9] M. Aidelsburger, M. Atala, M. Lohse, J. T. Barreiro, B. Paredes, and I. Bloch, *Phys. Rev. Lett.* **111**, 185301 (2013).
- [10] H. Miyake, G. A. Siviloglou, C. J. Kennedy, W. C. Burton, and W. Ketterle, *Phys. Rev. Lett.* **111**, 185302 (2013).
- [11] M. Atala, M. Aidelsburger, M. Lohse, J. T. Barreiro, B. Paredes, and I. Bloch, *Nat. Phys.* **10**, 588 (2014).
- [12] C. J. Kennedy, W. C. Burton, W. C. Chung, and W. Ketterle, *Nat. Phys.* **11**, 859 (2015).
- [13] M. E. Tai, A. Lukin, M. Rispoli, R. Schittko, T. Menke, D. Borgnia, P. M. Preiss, F. Grusdt, A. M. Kaufman, and M. Greiner, *Nature (London)* **546**, 519 (2017).
- [14] T. Oka and H. Aoki, *Phys. Rev. B* **79**, 081406(R) (2009).
- [15] T. Kitagawa, T. Oka, A. Brataas, L. Fu, and E. Demler, *Phys. Rev. B* **84**, 235108 (2011).
- [16] N. H. Lindner, G. Refael, and V. Galitzki, *Nat. Phys.* **7**, 490 (2011).
- [17] J. Cayssol, B. Dóra, F. Simon, and R. Moessner, *Phys. Status Solidi RRL* **7**, 101 (2013).
- [18] W. Zheng and H. Zhai, *Phys. Rev. A* **89**, 061603(R) (2014).
- [19] G. Jotzu, M. Messer, R. Desbuquois, M. Lebrat, T. Uehlinger, D. Greif, and T. Esslinger, *Nature (London)* **515**, 237 (2014).
- [20] S. K. Baur, M. H. Schleier-Smith, and N. R. Cooper, *Phys. Rev. A* **89**, 051605(R) (2014).
- [21] M. Aidelsburger, M. Lohse, C. Schweizer, M. Atala, J. T. Barreiro, S. Nascimbéne, N. R. Cooper, I. Bloch, and N. Goldman, *Nat. Phys.* **11**, 162 (2015).
- [22] N. Fläschner, B. S. Rem, M. Tarnowski, D. Vogel, D.-S. Lühmann, K. Sengstock, and C. Weitenberg, *Science* **352**, 1091 (2016).
- [23] M. Tarnowski, F. Nurüinal, N. Fläschner, B. S. Rem, A. Eckardt, K. Sengstock, and C. Weitenberg, *Nat. Commun.* **10**, 1728 (2019).
- [24] L. W. Clark, B. M. Anderson, L. Feng, A. Gaj, K. Levin, and C. Chin, *Phys. Rev. Lett.* **121**, 030402 (2018).
- [25] F. Görg, K. Sandholzer, J. Minguzzi, R. Desbuquois, M. Messer, and T. Esslinger, *Nat. Phys.* **15**, 1161 (2019).
- [26] C. Schweizer, F. Grusdt, M. Berngruber, L. Barbiero, E. Demler, N. Goldman, I. Bloch, and M. Aidelsburger, *Nat. Phys.* **15**, 1168 (2019).
- [27] L. W. Clark, A. Gaj, L. Feng, and C. Chin, *Nature (London)* **551**, 356 (2017).
- [28] L. Feng, J. Hu, L. W. Clark, and C. Chin, *Science* **363**, 521 (2019).
- [29] Z. Wu and H. Zhai, *Phys. Rev. A* **99**, 063624 (2019).
- [30] J. Hu, L. Feng, Z. Zhang, and C. Chin, *Nat. Phys.* **15**, 785 (2019).
- [31] E. L. Hahn, *Phys. Rev.* **80**, 580 (1950).
- [32] H. Y. Carr and E. M. Purcell, *Phys. Rev.* **94**, 630 (1954).
- [33] Y. Castin and R. Dum, *Phys. Rev. Lett.* **79**, 3553 (1997).
- [34] M. M. Maricq, *Phys. Rev. B* **25**, 6622 (1982).
- [35] N. Goldman and J. Dalibard, *Phys. Rev. X* **4**, 031027 (2014).
- [36] N. Goldman, J. Dalibard, M. Aidelsburger, and N. R. Cooper, *Phys. Rev. A* **91**, 033632 (2015).
- [37] See Supplemental Material at <http://link.aps.org/supplemental/10.1103/PhysRevA.102.011301> for the justification of the use of the effective 1D Hamiltonian and the dependence of many-body echo on various system parameters.
- [38] B. Swingle, G. Bentsen, M. Schleier-Smith, and P. Hayden, *Phys. Rev. A* **94**, 040302(R) (2016).
- [39] G. Zhu, M. Hafezi, and T. Grover, *Phys. Rev. A* **94**, 062329 (2016).
- [40] H. Shen, P. Zhang, R. Fan, and H. Zhai, *Phys. Rev. B* **96**, 054503 (2017).
- [41] J. Grond, A. I. Streltsov, and L. S. Cederbaum, *Phys. Rev. A* **86**, 063607 (2012).
- [42] J. Grond, A. I. Streltsov, A. U. J. Lode, K. Sakmann, L. S. Cederbaum, and O. E. Alon, *Phys. Rev. A* **88**, 023606 (2013).
- [43] J. H. V. Nguyen, M. C. Tsatsos, D. Luo, A. U. J. Lode, G. D. Telles, V. S. Bagnato, and R. G. Hulet, *Phys. Rev. X* **9**, 011052 (2019).